



## Biomarkers

# Over-expression of PD-1 Does Not Predict Leukemic Relapse after Allogeneic Stem Cell Transplantation



Prachi Jain<sup>1</sup>, Xin Tian<sup>2</sup>, Stefan Cordes<sup>1</sup>, Jinguo Chen<sup>3</sup>, Caroline R. Cantilena<sup>1</sup>, Christian Bradley<sup>1</sup>, Reema Panjwani<sup>1</sup>, Fariba Chinian<sup>1</sup>, Keyvan Keyvanfar<sup>1</sup>, Mino Battiwalla<sup>1</sup>, Pawel Muranski<sup>1</sup>, A. John Barrett<sup>1</sup>, Sawa Ito<sup>1,\*</sup>

<sup>1</sup> Hematology Branch, National Heart, Lung, and Blood Institute, National Institutes of Health, Bethesda, Maryland

<sup>2</sup> Office of Biostatistics Research, National Heart, Lung, and Blood Institute, National Institutes of Health, Bethesda, Maryland

<sup>3</sup> Center for Human Immunology, Autoimmunity, and Inflammation, National Institutes of Health, Bethesda, Maryland

### Article history:

Received 22 May 2018

Accepted 27 September 2018

### Key Words:

Post-transplant relapse

Biomarker

Graft-versus-leukemia effect

### ABSTRACT

Blockade of the T-cell exhaustion marker PD-1 to re-energize the immune response is emerging as a promising cancer treatment. Relapse of hematologic malignancy after allogeneic stem cell transplantation limits the success of this approach, and PD-1 blockade may hold therapeutic promise. However, PD-1 expression and its relationship with post-transplant relapse is poorly described. Because the donor immunity is activated by alloresponses, PD-1 expression may differ from nontransplanted individuals, and PD-1 blockade could risk graft-versus-host disease. Here we analyzed T-cell exhaustion marker kinetics and their relationship with leukemia relapse in 85 patients undergoing myeloablative T-cell-depleted HLA-matched stem cell transplantation. At a median follow-up of 3.5 years, 35 (44%) patients relapsed. PD-1 expression in CD4 and CD8 T cells was comparably elevated in relapsed and nonrelapsed cohorts. Helios<sup>+</sup> regulatory T cells and CD8 effector memory cells at day 30 emerged as independent predictors of relapse. Although leukemia antigen-specific T cells did not overexpress PD-1, single-cell analysis revealed LAG3 and TIM3 overexpression at relapse. These findings indicate that PD-1 is an unreliable marker for leukemia-specific T-cell exhaustion in relapsing patients but implies other exhaustion markers and suppressor cells as relapse biomarkers.

Published by Elsevier Inc. on behalf of American Society for Blood and Marrow Transplantation.

## INTRODUCTION

Relapse of primary disease is a major obstacle to successful allogeneic stem cell transplantation (allo-SCT) in hematologic malignancies [1–3]. The mechanisms underlying post-transplantation relapse are multifactorial and incompletely understood [4,5], but failure of the graft-versus-leukemia (GVL) effect may contribute to post-transplantation relapse [6]. There is a growing interest in PD-1 and other T-cell immune checkpoint markers as therapeutic targets for hematologic malignancies [7]. Early phase trials showed that immune checkpoint inhibitors can induce clinical responses in selected cases of post-transplantation relapse [8,9]. In allo-SCT, however, the immune checkpoint inhibitors can also induce severe, steroid-refractory graft-versus-host disease (GVHD) through activation of diverse alloreactive T-cell population irrespective of their contribution to GVHD or GVL [9].

Therefore, understanding PD-1 kinetics and its relationship to relapse is desirable before using checkpoint inhibitors to prevent or treat relapse after allo-SCT.

Here we evaluated the relationship between the kinetics of T-cell checkpoint markers and leukemia relapse in the early post-transplantation period. We further analyzed the leukemia-associated antigen (LAA)-specific T cells and T-cell exhaustion markers at relapse and sought to define the status of donor T cells at relapse at the single-cell level.

## METHODS

### Clinical Study Design

Eighty-five patients with various hematologic malignancies received ex vivo T-cell-depleted HLA-matched related sibling allo-SCT at a single center between 2006 and 2015. All patients signed an informed consent before enrollment, and the study was conducted in compliance with the Declaration of Helsinki under the protocols approved by the Institutional Review Board of the National Heart, Lung, and Blood Institute (Clinicaltrial.gov ID: NCT00378534, NCT01517035, and NCT01866839). All subjects received a myeloablative conditioning regimen of cyclophosphamide, fludarabine, and total body irradiation (600 to 1200 cGy) with GVHD prophylaxis of low-dose cyclosporine until day 21 (target trough level between 100 and 200 ng/mL). Peripheral blood stem cells with G-CSF mobilization were used as a graft source, and ex vivo T-cell depletion was performed either by CD3<sup>+</sup>/CD19<sup>+</sup> cell depletion (n = 20) or CD34<sup>+</sup> cell selection (n = 65) using Miltenyi CliniMACS

*Financial disclosure:* See Acknowledgments on page 222.

\* Correspondence and reprint requests: Sawa Ito, MD, Hematology Branch, National Heart, Lung, and Blood Institute, National Institutes of Health, 10 Center Drive, Building 10 CRC Room 5-3581, Bethesda MD 20892.

E-mail address: [itos2@mail.nih.gov](mailto:itos2@mail.nih.gov) (S. Ito).

<https://doi.org/10.1016/j.bbmt.2018.09.037>

1083-8791/Published by Elsevier Inc. on behalf of American Society for Blood and Marrow Transplantation.

magnetic selection system. Donor lymphocyte infusions were administered for 7 subjects who developed late-onset graft failure before day 100. Because donor lymphocyte infusions can affect the immune reconstitution, these 7 patients were excluded from clinical correlation analysis. Median percentages of CD3 T-cell chimerism were 91% at day 30, 98% at day 60, and 99% at day 100, respectively.

#### Laboratory Study Design

##### Sample collections and storage

Peripheral blood was collected from the donors, and from the recipients, pretransplantation, at days 30, 60, and 100 after allo-SCT. Additional blood was collected around the time of relapse from relapsing patients. Peripheral blood mononuclear cells (PBMCs) were isolated by Ficoll-Hypaque density-gradient centrifugation and cryopreserved in liquid nitrogen until further use.

##### Flow cytometry phenotype analysis

Multicolor flow cytometric analysis was performed to characterize T-cell subsets, memory T cells, helper T cells, regulatory T cells (T<sub>regs</sub>) with T-cell checkpoint markers (PD-1, TIM-3, and LAG3). Briefly, the cells were first stained with fixable violet live-dead dye (Vivid; Invitrogen, Carlsbad, CA) for 15 minutes, followed by staining for chemokine receptor at 37°C and other cell surface markers for 15 minutes at room temperature. For intracellular staining, the cells were further permeabilized using Foxp3 fixation/permeabilization buffer (eBioscience, San Diego, CA) for 30 minutes at 4°C followed by 30 minutes' incubation with intracellular antigen antibodies at room temperature. T-cell memory subsets were determined within either CD4 or CD8 T-cell population to identify naive cells (CCR7+CD45RO-), central memory cells (CCR7+CD45RO+), effector memory cells (CCR7-CD45RO-), and effector memory RA (TEMRA; CCR7-CD45RO-CD27-CD45RA+). PD-1-positive cell population were determined within the CD4 population based on fluorescence minus one control. Regulatory T-cell subsets were identified within the CD4 T-cell population based on the expression of 2 transcription factors, FoxP3 and Helios. Antibodies used in the flow cytometry experiment were summarized in Supplementary Table S1, and the gating strategy of flow cytometry was summarized in Supplementary Figure S1. The data acquisition was performed using a Becton Dickinson LSRII Fortessa (BD Biosciences, San Jose, CA) and analyzed using FlowJo software (Tree Star Inc, Ashland, OR). At least 20,000 events per CD3±T cell population were acquired on a Becton Dickinson LSRII Fortessa cytometer to ensure a sufficient number of cells for statistical analysis. Data were analyzed using FlowJo software version 10 (Tree Star Inc).

##### Antigen-specific T-cell detection

**Virus- and leukemia-associated antigen peptides.** Pooled PepMix HIV-1 (Con B gag motif; JPT, Berlin, Germany) was used as a negative control antigen and OKT3 (anti-human CD3, functional grade purified, eBioscience) was used as a positive control for both ELISPOT and flow cytometry-based antigen-specific T-cell assay. The following peptides were used as target antigens: cytomegalovirus (PepMix HCMVA, pp65; JPT), PRAME (PepMix Human Prame/OIP4; JPT), MAGEA3 (Pepmix Human MAGEA3; JPT), NYESO (PepMix Human NY-ESO-1; JPT), WT1 (PepTivator WT1—premium grade; Miltenyi Biotec, Bergisch Gladbach, Germany), and Aurora kinase (Custom-made PepTrack-Peptide Libraries; JPT).

**Enzyme-linked immunospot assay.** Enzyme-linked immunospot assay was performed using the human IFN $\gamma$ /TNF- $\alpha$ /IL-2 Three-Color Fluorospot kit (Cellular Technology Limited, Cleveland, OH) under the guidance of the manufacturer's instruction. After thawing PBMC in serum-free AIM-V medium, the cells were plated at 200,000 cells/well in duplicates. Then cells were stimulated with peptides at a concentration of 1  $\mu$ g/ml without any additional antigen-presenting cells and incubated at 37°C 5% CO<sub>2</sub> for 20 hours. The plates were scanned using ImmunoSpot Series 6 Analyzer (CTL, Shaker Heights, OH) and analyzed using ImmunoSpot 6.0 software (CTL) with either basic count or smart count mode, and gating was autoadjusted depending on positive control wells and negative control wells.

**Flow cytometry.** PBMC were thawed in serum-free AIM-V medium, washed and cultured with individual peptides in. In a 96-well round-bottom cell plate, 2  $\times$  10<sup>5</sup> cells (50  $\mu$ L) were stimulated with each individual peptide (1  $\mu$ g/ml; 50  $\mu$ L) in the presence of costimulatory anti-human CD28 (clone CD28.2), anti-human CD49d (clone 9F10), and protein transport inhibitor Golgi stop (Cat-51-2092KZ; BD Bioscience), Golgi plug (Cat-51-2301KZ; BD Bioscience) and AIM-V medium. The plate was incubated at 37°C in a humidified incubator maintained at 5% CO<sub>2</sub> for 6 hours. After a 6-hour incubation period, the plates were stained with fixable violet live-dead dye (Vivid, Invitrogen) for 15 minutes at 4°C, followed by staining for chemokine receptor at 37°C and then for cell surface markers for 15 minutes at room temperature. For intracellular staining, cells were fixed and permeabilized (BD Cytofix/Cytoperm Kit; BD Biosciences) for 45 minutes at 4°C in dark. After washing with Perm/Wash solution (BD Cytofix/Cytoperm Kit; BD Biosciences), cells were stained intracellularly with the antibodies in 50  $\mu$ L Perm/Wash buffer

for 30 minutes at room temperature in the dark. Stained cells were acquired on a Becton Dickinson LSRII Fortessa cytometer (BD Biosciences), and data were analyzed using FlowJo software version 10 (Tree Star Inc).

**Leukemia-associated antigen RT-PCR.** Relative changes in RNA expressions of leukemia associated antigens were evaluated by RT-PCR array. RNA was extracted from bulk peripheral blood using the All prep DNA/RNA Mini kit (Qiagen, Hilden, Germany) according to the manufacturer's instructions. To synthesize cDNAs, 1  $\mu$ g of RNA was reverse transcribed using the iScript gDNA clear cDNA synthesis kit (Bio-Rad Laboratories, Hercules, CA), according to manufacturer's instruction. The RT-PCR reactions were performed using 5 ng cDNA and SsoAdvanced Universal SYBR green Supermix (Bio-Rad Laboratories) in custom-made 384-well plate PrimePCR Assay Panels for Real-Time PCR (8 target genes; Bio-Rad Laboratories; Supplementary Table S2) in 7500 Real Time PCR system (Applied Biosystems, Foster City, CA). The PCR was run for 2 minutes at 95°C for 1 cycle (activation), followed by 40 cycles of 95°C for 5 seconds (denaturation), 40 cycles of 60°C for 30 seconds (annealing), and then melt curve step of 65°C to 95°C increment (5 seconds/step) for 1 cycle. Glyceroldehyde 3-phosphate dehydrogenase, ABL1 and ACTB (Actin) were used as housekeeping genes.

**Flow sorting of antigen-specific T cells.** In a 24-well flat-bottom plate, 10 million cells/mL/well were stimulated for 6 hours with peptides libraries of PRAME or CMVpp65 in the presence of costimulatory CD28/CD49d. After the 6-hour incubation, the cells were collected from each well, and TNF $\alpha$  secretion assay was performed using Cell enrichment and Detection (PE) human kit (Miltenyi Biotec) per manufacturer's instructions to detect PRAME or CMVpp65-specific T cells. Dead cells were excluded using fixable violet live-dead dye (Vivid; Invitrogen) by staining for 15 minutes at 4°C. The following antibody clones were used for staining: TNF $\alpha$  detection PE (MACS Miltenyi, provided with kit), CD3 BV605 (Biolegend, clone 317322), CD14-CD19-Pacific Blue (Clone MHCD1428 and MHCD1928, respectively; Life Technologies) as dump channel and acquired on flow for sorting. TNF $\alpha$ -positive and TNF $\alpha$ -negative populations were sorted using FACS sorter ARIA II (BD Bioscience).

**Single-cell RNA-seq.** Single-cell 3' digital gene expression profiling for CMVpp65- or PRAME-specific T cells was performed via the 10x Chromium Single Cell Platform (10x Genomics, Pleasanton, CA) at a targeted cell number of 5000 cells. Single cell RNA-seq libraries generation, GEM-RT, and cDNA amplification were performed according to the manufacturer's instructions, and libraries were sequenced on Illumina HiSeq 3000 (Illumina, San Diego, CA).

#### Statistical Analysis

The data from RT-PCR assays were analyzed with Prime PCR software (Bio-Rad Laboratories). Cumulative incidences of relapse were estimated and compared by the Gray's method, which adjusts for competing risks due to nonrelapse mortality [10]. Overall survival and postrelapse survival probabilities were estimated by the Kaplan-Meier method and compared between subgroups of patients by the log-rank test. Comparisons were carried out between patients who relapsed and those did not relapse. For comparing categorical variables and continuous variables between relapsed and nonrelapsed cohorts, Fisher's exact test and Mann-Whitney test were used, respectively. Multivariate analysis based on the Cox proportional hazards regression was used to examine the risk factors for the cause-specific hazards of relapse controlling for pre-transplant characteristics. All tests were 2-sided and *P* values <.05 were considered statistically significant. Analysis were performed using the R statistical software, version 3.4.3 (R Foundation for Statistical Computing, Vienna, Austria) and graphs were generated using Prism 5.03 (GraphPad Software, Inc., La Jolla, CA).

The Cell Ranger Single-Cell Software was used for sample demultiplexing, barcode processing, single-cell gene counting, and cell clustering. The Database for Annotation, Visualization, and Integrated Discovery (DAVID version 6.8; HYPERLINK "https://david.ncifcrf.gov/home.jsp") [11] was used for Gene Ontology annotation analysis of Biological Process in the set of genes passing threshold (fold changes > 2.0 and *P* < .05) in each cluster.

## RESULTS

### Post-Transplantation Outcomes

At a median follow-up of 3.5 years, 35 of 85 patients had relapsed with a 10-year cumulative relapse incidence of 44% and a median time to relapse of 226 days (range, 33 to 1774) after transplantation (Figure 1A). Overall survival was significantly poorer in the relapsed patients compared with nonrelapsed patients (*P* < .001), and most of the relapsed patients (92%) died of relapse or its complications. Postrelapse survival was significantly inferior among subjects relapsing before

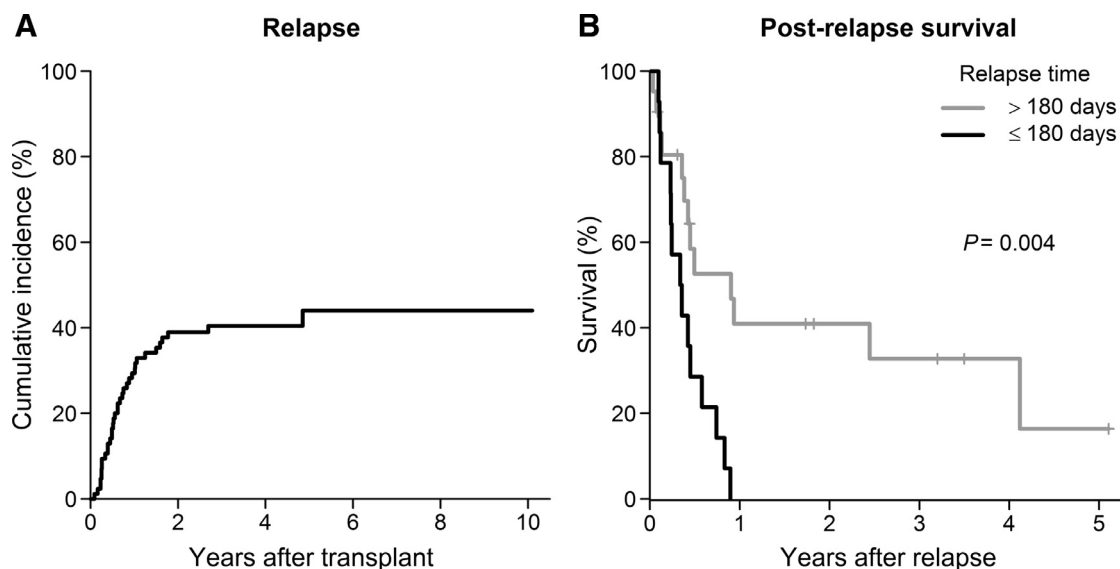


**Figure 1.** (A) Cumulative incidence of relapse. (B) Kaplan-Meier estimate of postrelapse survival in subjects with the time to relapse > 180 versus ≤ 180 days.

180 days after allo-SCT (median postrelapse survival of 126 days versus 329 days for patients relapsing after 180 days;  $P = .004$ , Figure 1B). There was no difference of the relapse incidences among 3 clinical protocols ( $P = .94$ ). Other transplant parameters were similar between relapsed and nonrelapsed subjects, including recipient age, donor age, donor-recipient gender mismatch, diagnosis, disease risk, cytomegalovirus (CMV) reactivation, acute or chronic GVHD (Supplementary Table S3).

#### Early T-Cell Reconstitution and Relapse

To investigate whether T cell reconstitution in the early post-transplant phase affected the relapse incidence and outcome, we analyzed T cell memory subset,  $T_{\text{regs}}$ , and PD-1 expression in both CD4 and CD8 T cells in the donor and at day 30, day 60, and day 100 after allo-SCT.

Post-transplantation PD-1 expression in CD4 and CD8 T cells was significantly and comparably elevated in both relapsed and non-relapsed cohorts when compared to donors (Figure 2A,B). No association was observed between relapse incidence and pattern of PD-1 expression. In contrast, %Helios<sup>+</sup> $T_{\text{regs}}$  was significantly higher in the relapsed cohort at day 30 ( $P = .01$ , Figure 2C).

Absolute numbers of each subpopulation of T cells were also analyzed. Although absolute number of PD-1<sup>+</sup> CD4 cells was similar between the cohorts (Figure 2D), absolute PD-1<sup>+</sup> CD8 cells were significantly higher at day 30 ( $P = .03$ ) in the relapsed cohort (Figure 2E). However, absolute PD-1<sup>+</sup> CD8 number was significantly correlated to absolute number of effector memory (EM) CD8 cells, which was significantly higher in the relapsed cohort at all time points in the early post-transplantation period ( $P < .05$ ; Figure 2F).

#### Predictive Biomarkers of T-Cell Reconstitution for Relapse

In multivariate analysis using either continuous or dichotomized variables, %Helios<sup>+</sup>  $T_{\text{regs}}$  CD4 cell and absolute number of CD8 effector memory cells at day 30 were identified as independent biomarkers predicting relapse (Supplementary Table S4). %Helios<sup>+</sup> $T_{\text{regs}}$  CD4 cells greater than 10% of CD4 cells and absolute number of CD8 effector memory cells greater than 150/ $\mu\text{L}$  at day 30 were significantly associated with a higher risk and earlier incidence of relapse ( $P = .003$  and  $P = .008$ , respectively;

Figure 3A, 3B, and Supplementary Figure S2). PD-1 expression did not predict the incidence of relapse in this cohort. In the Cox regression analysis with GVHD as a time-dependent covariate, we found that neither incidence nor severity of acute or chronic GVHD was significantly associated with relapse ( $P > .10$ , Supplementary Table S3). Furthermore, %Helios<sup>+</sup> $T_{\text{regs}}$  or the effector memory CD8 T cells were not significantly associated with acute or chronic GVHD ( $P > .10$ ).

#### PD-1 and Other T-Cell Exhaustion Markers at Relapse

In 24 of 35 relapsed subjects where blood samples were saved at the time of relapse, we analyzed PD-1, LAG3, TIM-3, PDL-1 expressions in both CD4 and CD8 T cells, compared with the corresponding pretransplant donor samples. The median time from the transplant to relapse was 183 days in these 24 individuals. Compared with donors, the proportion of PD-1 expressing cells were significantly higher in both CD4 and CD8 T cells in relapsed patients (mean %PD-1<sup>+</sup> CD4 cells,  $17.7 \pm 7.2$  in donor versus  $65.8 \pm 18.5$  in relapsed patients,  $P < .0001$ ; mean %PD-1<sup>+</sup> CD8 cells,  $16.4 \pm 9.5$  in donors versus  $41.3 \pm 25.5$  in relapsed patients,  $P < .0001$ ). The increased expressions of PD-1 were observed in all compartments of CD4 and CD8 T cell memory subsets including naive and stem cell memory subset (Figure 4A,E). In contrast, differential expressions of LAG3, TIM3, and PDL-1 expressions were limited to certain memory subsets (Figure 4B-D,F-H). This observation suggests that high PD-1 expressions in T cells persisted at the time of post-transplantation relapse and was present even in the early stages of T-cell maturation. Other T-cell exhaustion markers (LAG3, TIM3, and PDL-1) appeared to have a more distinct phenotype at leukemia relapse.

#### Leukemia-Associated Antigen-Specific T Cells

To explore the role of PD-1 expressions in GVL effects, we further analyzed 6 relapsed subjects (5 AML, 1 ALL) for blast cell expression of 5 LAA (AURAK, NY-ESO1, MAGEA3, PRAME, WT1) and corresponding T cells specific to these LAA. PBMCs from relapsed patients expressed at least 1 and up to 4 LAA by RT-PCR before and after relapse in all patients. LAA-specific T cells were observed in 4 subjects by Elispot; however, all relapsed samples eventually expressed new LAA different from those targeted by their own LAA-specific T cells,

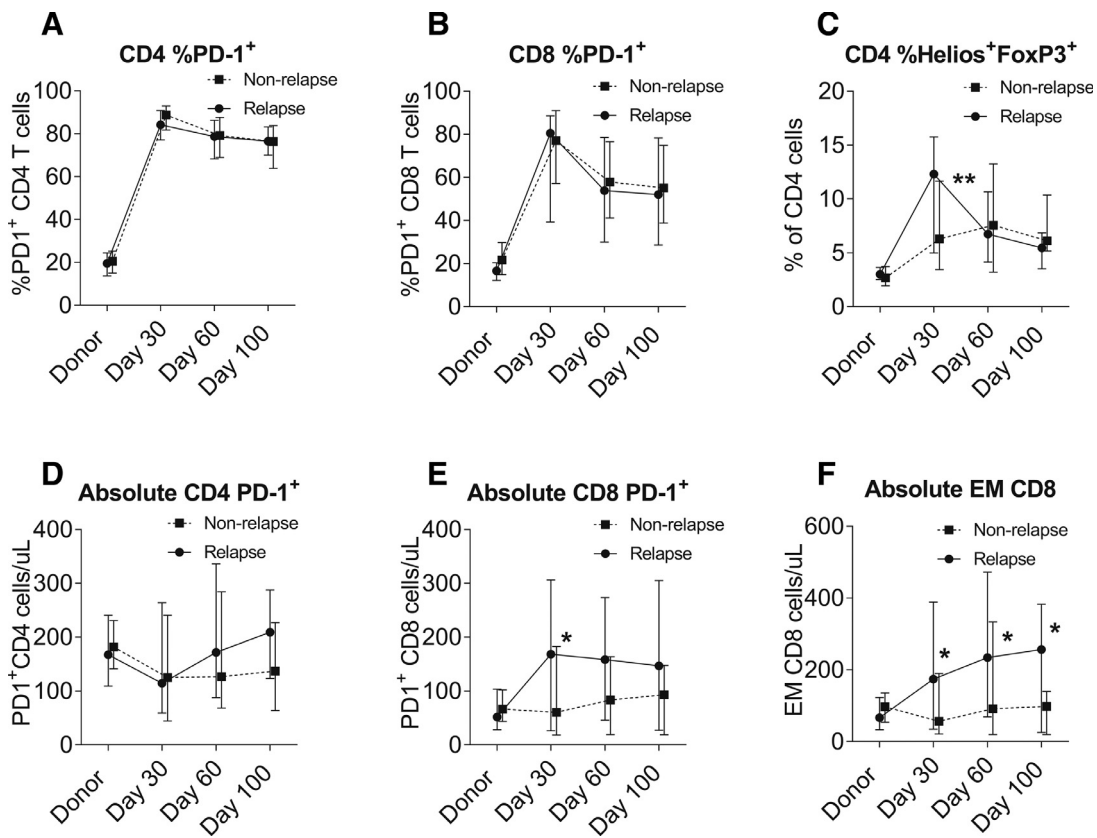


**Figure 2.** Comparison of cellular immune subsets between the relapsed and nonrelapsed cohorts. (A) Percentages of PD-1<sup>+</sup> in CD4 cells. (B) Percentages of PD-1<sup>+</sup> in CD8 cells. (C) Percentages of Helios<sup>+</sup>FoxP3<sup>+</sup> in CD4 cells. (D) Absolute numbers of PD-1<sup>+</sup>CD4 cells. (E) Absolute numbers of PD-1<sup>+</sup>CD8 cells. (F) Absolute numbers of effector memory CD8 cells.

suggesting immunologic escape of leukemic blasts (Figure 5A). In UPN1 and UPN3, PRAME-specific T cells were also measurable by flow cytometry at the time of relapse. Although CMV-specific T cells were enriched in PD-1 positive fractions, PRAME-specific T cells were disproportionately detected in the PD-1 negative fractions (Figure 5B). This implies that the PD-1 overexpression at relapse was more likely to be derived from T cells specific for viruses or other chronically exposed antigen and was unlikely from leukemia-specific T cells.

**Single Cell RNA-seq Analysis of PRAME and CMV-Specific T Cells at Relapse**

Next, we performed single-cell RNA-seq analysis of T cells specific to virus or leukemia from UPN1 sample at relapse. Briefly, PBMC were stimulated with peptide pools of either CMVpp65 or PRAME, then both TNF $\alpha$ -positive and -negative fractions of T cells were sorted by flow cytometry for single-cell transcriptome analysis. An average of 1436 cells per condition were analyzed with mean reads number of 381,079 per cell and median gene number of 1091 per cell. Cluster analysis of the

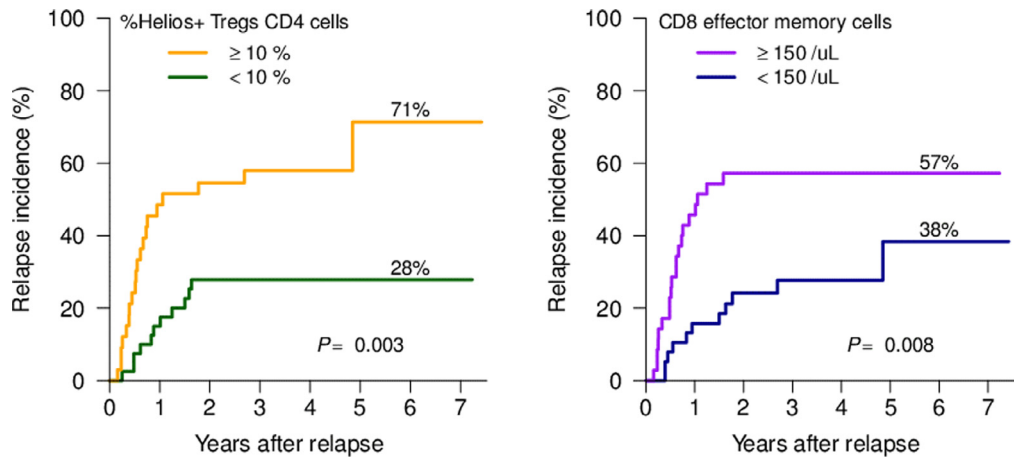


**Figure 3.** Cumulative incidence of relapse in (A) subjects with %Helios<sup>+</sup>T<sub>regs</sub> CD4 cells at day 30 <10% versus ≥ 10%. (B) Subjects with absolute number of CD8 effector memory cells at day 30 <150/uL versus ≥ 150/uL.

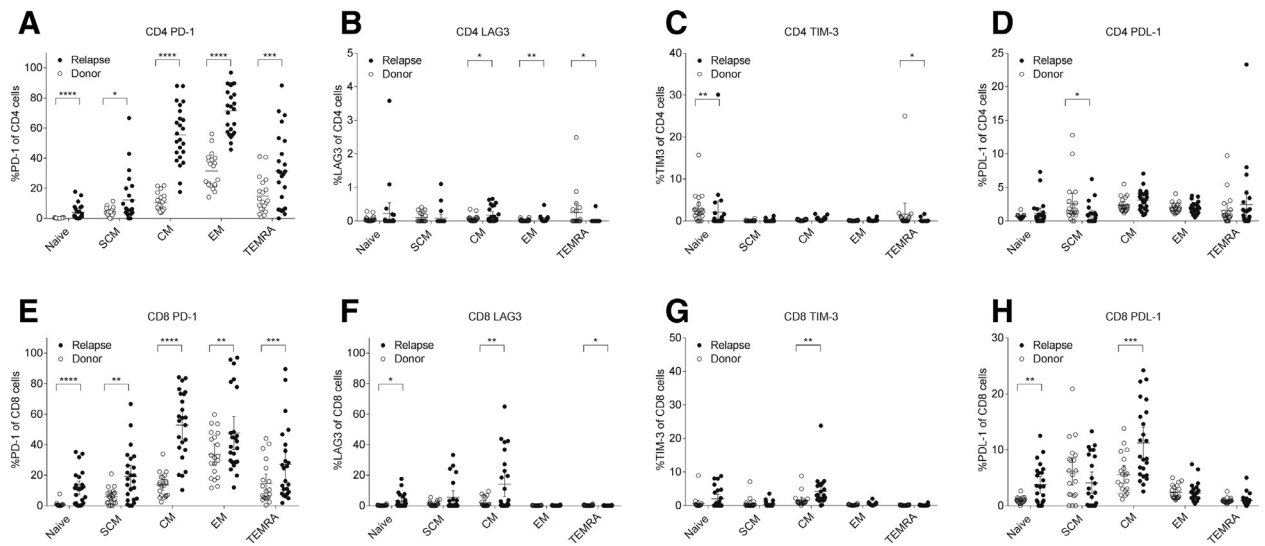


**Figure 4.** Comparison of exhaustion marker expressions in T-cell memory subsets between the relapsed cohort and paired donor cohorts. (A) Percentages of PD-1<sup>+</sup> in CD4 cells. (B) Percentages of LAG3<sup>+</sup> in CD4 cells. (C) Percentages of TIM-3<sup>+</sup> in CD4 cells. (D) Percentages of PDL-1<sup>+</sup> in CD4 cells. (E) Percentages of PD-1<sup>+</sup> in CD8 cells. (F) Percentages of LAG3<sup>+</sup> in CD8 cells. (G) Percentages of TIM-3<sup>+</sup> in CD8 cells. (H) Percentages of PDL-1<sup>+</sup> in CD8 cells.

4 pooled samples (CMVpp65 positive or negative and PRAME positive or negative) revealed heterogeneous population of 13 clusters (Figure 6A). Clusters were roughly classified into 3 categories that predominantly consisted of (1) CMVpp65- and PRAME-positive T cells (clusters 2, 6, 9, 10, 11 shown in red box), (2) CMVpp65- and PRAME-negative T cells (clusters 1, 3, 7, 8, 13 shown in blue box), and (3) nonspecific T cells (cluster 4, 5, 12 shown in orange box) (Figure 6B). Among the clusters of antigen-reactive T cells, Gene Ontology analyses confirmed that cluster 2 was enriched for the genes involved with TNF-receptor-mediated signaling pathway. Cluster 9 and 11 have distinct gene signatures related to cell division, DNA replication, mitotic nuclear division, and sister chromatid cohesion, suggesting an actively proliferating T-cell population (Supplementary Table S5). Individual gene analysis at a single-cell level revealed that

*PDCD1* (PD-1) was barely expressed in PRAME-reactive T cells. In contrast, *LAG3* and *HAVCR2* (TIM3) were highly expressed in the activated T-cell portion of PRAME-reactive T cells but not in CMV-reactive T cells (Figure 6C). The observation was consistent with flow cytometry analysis that PRAME-reactive T cells were predominantly enriched in the PD-1-negative fraction in this subject.

## DISCUSSION

Post-transplantation relapse remains the major cause of transplant failure, occurring in 20% to 40% of standard-risk patients and in 40% to 80% of high-risk patients and accounting for more than half of deaths after allo-SCT [1,12]. Outcomes of post-transplantation relapse are extremely poor with 1-year and 3-year overall survival rates of 22% and <10%, respectively

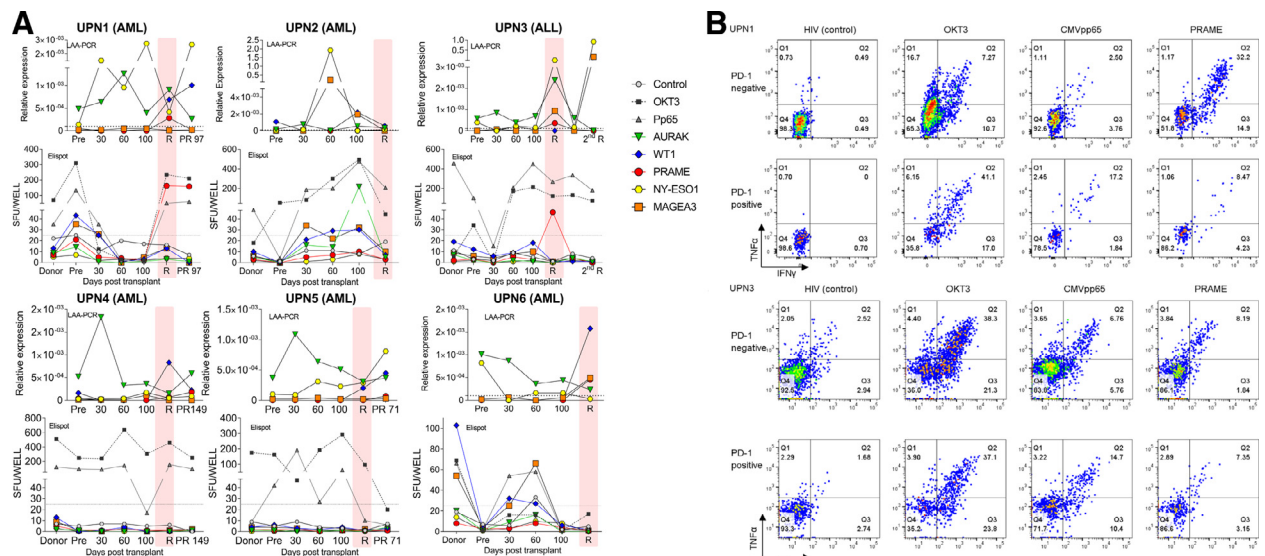


**Figure 5.** (A) Correlation between LAA and antigen-specific T cells in 6 subjects. Five LAAs (AURAK, NY-ESO1, MAGEA3, PRAME, WT1) were quantified in peripheral blood by reverse transcription polymerase chain reaction and leukemia-specific T cells were simultaneously measured by enzyme-linked immunosorbent spot-forming cell assay. (B) Representative flow data of antigen-specific T cells in PD-1 negative or positive fractions (UPN1 and UPN3). HIV was used as negative control and OKT3 as positive control.

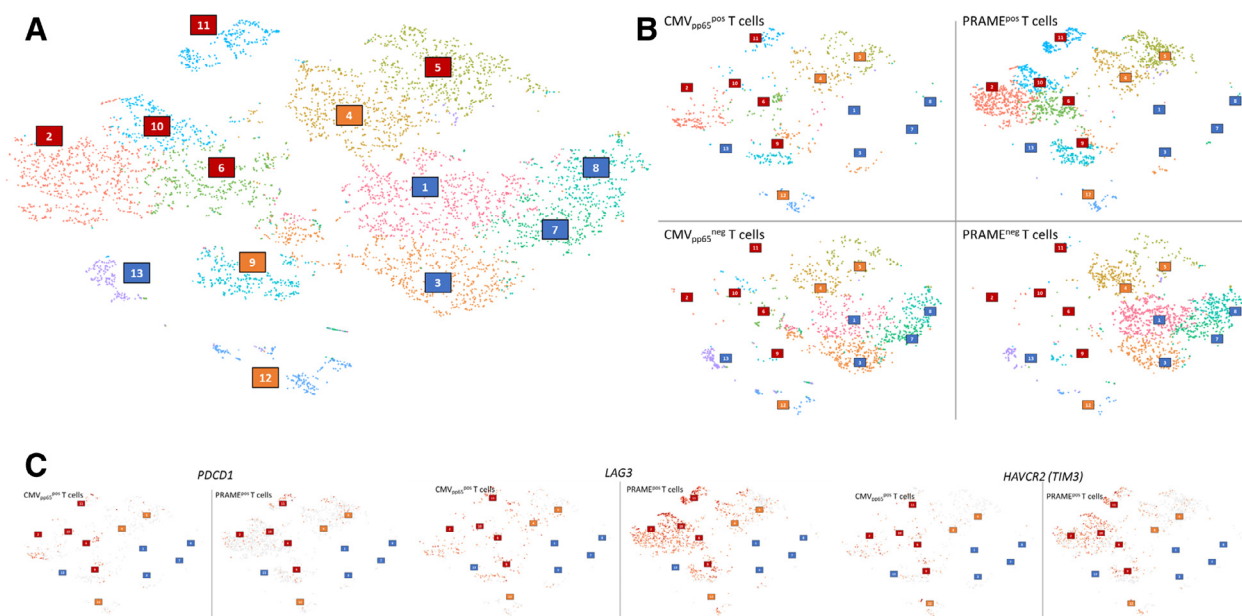


**Figure 6.** Single-cell RNA-seq analysis of PRAME- and CMVpp65-specific T cells at relapse in UPN1. (A) Cluster analysis of the 4 pooled samples. Clusters were roughly classified into 3 categories: CMVpp65- and PRAME-positive T cells, clusters 2, 6, 9, 10, 11 shown in red boxes; CMVpp65 and PRAME negative T cells, clusters 1, 3, 7, 8, 13 shown in blue boxes; and nonspecific T cells, cluster 4, 5, 12 shown in orange boxes. (B) Cluster analysis of each 4 samples: CMVpp65-positive or -negative cells and PRAME-positive or -negative cells. (C) Comparison of expression profiles of exhaustion markers in CMVpp65- and PRAME-positive T cells at a single cell level. *PDCD1* (PD-1) on the left, *LAG3* in the middle, and *HAVCR2* (*TIM3*) on the right.

[2,13]. There is an urgent need to prevent and treat post-transplantation relapse through new strategies to enhance GVL effects without inducing severe GVHD. To optimize immunologic approaches to prevent and treat relapse, we studied the kinetics of suppressive markers of cellular immunity after allo-SCT and its relationship to the incidences of subsequent relapse.

In this study, we found that PD-1 was ubiquitously overexpressed in T cells during the early post-transplantation period and PD-1 expression patterns did not selectively identify patients destined to relapse. We further showed that PD-1 was not overexpressed in the leukemia antigen-specific T cells, rather PD-1 positive fractions were enriched with CMV-specific T cells. This observation is consistent with the previous report of Gallez-Hawkins et al [14] demonstrating enhanced PD-1 expression during CMV reactivation and severe GVHD after allo-SCT. In another report, high PD-1 expression in CD4 cells was associated with non-survivors in allo-SCT of various stem cell sources [15]. Therefore, PD-1 blockade after allo-SCT may be a double-edged sword promoting antiviral immunity but inducing severe GVHD without increasing GVL effects. Finally, single-cell analysis revealed LAG3 and TIM3 overexpression in PD-1-negative PRAME-specific T cells. This preliminary result implies possible roles for other exhaustion markers in the mechanisms of post-transplantation relapse. Alternatively, lack of PD-1 expression indicates that PRAME-specific T cells may not have been fully functional in this subject because PD-1 is also recognized as a marker of T-cell activation.

In contrast to the indiscriminate expression of PD-1 in all post-transplantation patients irrespective of relapse status, 2 independent biomarkers at day 30 post-transplantation, Helios<sup>+</sup> T<sub>regs</sub> CD4 cells and absolute number of CD8 effector memory cells were strongly associated with higher incidence of relapse. Helios is a key transcription factor in T<sub>regs</sub> that stabilizes the functions of T<sub>regs</sub> through STAT5 activation [16] and epigenetically silencing *IL-2* expression [17]. Nakagawa et al [18] recently reported that selective deletion of Helios in CD4

T<sub>regs</sub> enhanced anti-tumor immunity in a mouse model, suggesting that Helios<sup>+</sup> T<sub>regs</sub> CD4 cells favor a permissive microenvironment for solid tumor growth. In allo-SCT, however, the roles of Helios<sup>+</sup> T<sub>regs</sub> in pathogenesis of GVHD and GVL remain undefined [19,20], and further studies are needed to validate Helios as a biomarker of post-transplantation relapse and as a potential therapeutic target.

There are several limitations in this study. First, our observation was limited to ex vivo T-cell-depleted matched-related donor allo-SCT after a TBI-based myeloablative conditioning regimen. The kinetics of post-transplantation PD-1 expressions may differ according to the donor type, graft source, conditioning regimen, GVHD prophylaxis, and post-transplantation therapy. Further study is needed to validate our findings in a larger cohort. Second, we only evaluated LAG3, TIM3, and PDL-1 at relapse and not in early post-transplantation samples. Smaller cohort study showed the higher expressions of PD-1 and TIM-3 in relapsed subjects (n = 5) in comparison to nonrelapsed subjects (n = 6) at various timepoints after allo-SCT [21]. However, we cannot assume that other exhaustion markers reliably predict post-transplantation relapse. Third, antigen-specific T cells were analyzed only for commonly shared leukemia-associated antigens (AURAK, NY-ESO1, MAGEA3, PRAME, WT1). In HLA-matched allo-SCT, hematopoietic lineage-specific minor histocompatibility antigens (MiHA) are known to induce allo-immunity responsible for a GVL effect. Norde et al [22] previously reported impaired function of MiHA-specific T cells through PD-1/PDL-1 axis at post-transplantation relapse. In our cohort, we did not have information about the disparity at the level of single-nucleotide polymorphism in MiHA genes (HA-1, HA-2, LRH-1, HB-1, ACC-1/ACC-2, UTA2-1, HEATR-1, AAC-6) between donor and recipient. We therefore could not analyze T-cell populations specific to MiHA [23]. In solid tumors, neoantigen-specific T cells were reported to be enriched in PD-1-positive fractions in either tumor infiltrating lymphocytes or peripheral blood [24,25]. However, the somatic mutation burdens of acute leukemia are generally low,

so the potency of neoantigen-specific T cells in GVL remains undetermined. Lastly, single-cell RNAseq analysis was conducted in only 1 representative sample. Despite the fact that LAG3 and TIM3 seemed overexpressed in PRAME-specific T cells, single-cell RNAseq data could not distinguish whether these molecules expressed on the cell surface or intracellular compartment. The murine model suggested that LAG3 molecules were mainly stored intracellularly and rapidly translocated to the cell surface when T cells were activated [26]. Functional significance of both surface and intracellular expressions of LAG3 and TIM3 remain undetermined in leukemia-specific T cells. Although these findings cannot be generalized to all post-transplantation relapses, the case validated the lack of RNA expressions of PD-1 in PRAME-specific T cells, highlighting the heterogeneity of antigen-specific T cell populations at a single cell level. Further study is needed to define the diversity and heterogeneity of the T cell repertoire in post-transplantation relapse.

In conclusion, our findings do not support PD-1 being the predominate marker for leukemia-specific T cell exhaustion in relapsing patients post-transplant but instead identify other exhaustion markers and suppressor cells as indicators of relapse. Our study also illustrated the unmet need of understanding the GVL effects in human samples to develop rationale combination therapies of checkpoint inhibitors and other immunotherapies in hematologic malignancies after allo-SCT.

#### ACKNOWLEDGMENTS

We thank Tameem Ansari, Jodi Hanson, and Jaya Ghosh (Cellular Technology Limited, Shaker Heights, OH, USA) for their technical support. We also thank all patients who donated the samples to this study. This research was supported by the Intramural Research Program of the National Heart, Lung, and Blood Institute at the National Institutes of Health.

*Conflict of interest statement:* All authors declare no conflict of interest.

*Authorship statement:* P.J., A.J.B., and S.I. managed the study concept and design. P.J., S.C., J.C., C.R.C., C.B., R.P., F.C., and K.K. managed in vitro experiment and data collection. P.J., X.T., S.C., P.M., A.J.B., and S.I. managed analysis and interpretation of data. P.J., X.T., S.C., M.B., P.M., A.J.B., and S.I. drafted the manuscript. X.T., S.C., and S.I. managed the statistical analysis. M.B., P.M., A.J.B., and S.I. were responsible for clinical data collection. A.J.B. and S.I. obtained funding and were responsible for study supervision.

#### SUPPLEMENTARY MATERIALS

Supplementary material associated with this article can be found in the online version at doi:10.1016/j.bbmt.2018.09.037.

#### REFERENCES

- Barrett AJ, Battiwalla M. Relapse after allogeneic stem cell transplantation. *Expert Rev Hematol.* 2010;3:429–441.
- Frangoul H, Jagasia M. Relapse post hematopoietic SCT remains the Achilles heel for the field. *Bone Marrow Transplant.* 2014;49:997–998.
- Kekre N, Koreth J. Novel strategies to prevent relapse after allogeneic hematopoietic stem cell transplantation for acute myeloid leukaemia and myelodysplastic syndromes. *Curr Opin Hematol.* 2015;22:116–122.
- Miller JS, Warren EH, van den Brink MR, et al. NCI First International Workshop on the Biology, Prevention, and Treatment of Relapse after Allogeneic Hematopoietic Stem Cell Transplantation: report from the Committee on the Biology Underlying Recurrence of Malignant Disease following Allogeneic HSCT: Graft-versus-Tumor/Leukemia Reaction. *Biol Blood Marrow Transplant.* 2010;16:565–586.
- Cairo MS, Jordan CT, Maley CC, et al. NCI First International Workshop on the Biology, Prevention, and Treatment of Relapse after Allogeneic Hematopoietic Stem Cell Transplantation: report from the Committee on the Biological Considerations of Hematological Relapse following Allogeneic Stem Cell Transplantation Unrelated to Graft-versus-Tumor Effects: state of the science. *Biol Blood Marrow Transplant.* 2010;16:709–728.
- Barrett AJ. Understanding and harnessing the graft-versus-leukaemia effect. *Br J Haematol.* 2008;142:877–888.
- Xu-Monette ZY, Zhou J, Young KH. PD-1 expression and clinical PD-1 blockade in B-cell lymphomas. *Blood.* 2018;131:68–83.
- Davids MS, Kim HT, Bachireddy P, et al. Ipilimumab for patients with relapse after allogeneic transplantation. *N Engl J Med.* 2016;375:143–153.
- Haverkos BM, Abbott D, Hamadani M, et al. PD-1 blockade for relapsed lymphoma post-allogeneic hematopoietic cell transplant: high response rate but frequent GVHD. *Blood.* 2017;130:221–228.
- Gray RJ. A class of K-sample tests for comparing the cumulative incidence of a competitive risk. *Ann Stat.* 1988;16:1141–1154.
- Huang da W, Sherman BT, Lempicki RA. Systematic and integrative analysis of large gene lists using DAVID bioinformatics resources. *Nat Protoc.* 2009;4:44–57.
- Pavletic SZ, Kumar S, Mohty M, et al. NCI First International Workshop on the Biology, Prevention, and Treatment of Relapse after Allogeneic Hematopoietic Stem Cell Transplantation: report from the Committee on the Epidemiology and Natural History of Relapse following Allogeneic Cell Transplantation. *Biol Blood Marrow Transplant.* 2010;16:871–890.
- Bejanyan N, Oran B, Shanley R, et al. Clinical outcomes of AML patients relapsing after matched-related donor and umbilical cord blood transplantation. *Bone Marrow Transplant.* 2014;49:1029–1035.
- Gallez-Hawkins GM, Thao L, Palmer J, et al. Increased programmed death-1 molecule expression in cytomegalovirus disease and acute graft-versus-host disease after allogeneic hematopoietic cell transplantation. *Biol Blood Marrow Transplant.* 2009;15:872–880.
- Schade H, Sen S, Neff CP, et al. Programmed death 1 expression on CD4<sup>+</sup> T cells predicts mortality after allogeneic stem cell transplantation. *Biol Blood Marrow Transplant.* 2016;22:2172–2179.
- Kim HJ, Barnitz RA, Kreslavsky T, et al. Stable inhibitory activity of regulatory T cells requires the transcription factor Helios. *Science.* 2015;350:334–339.
- Baine I, Basu S, Ames R, Sellers RS, Macian F. Helios induces epigenetic silencing of IL2 gene expression in regulatory T cells. *J Immunol.* 2013;190:1008–1016.
- Nakagawa H, Sido JM, Reyes EE, Kiers V, Cantor H, Kim HJ. Instability of Helios-deficient Tregs is associated with conversion to a T-effector phenotype and enhanced antitumor immunity. *Proc Natl Acad Sci U S A.* 2016;113:6248–6253.
- Hirakawa M, Matos TR, Liu H, et al. Low-dose IL-2 selectively activates subsets of CD4<sup>+</sup> Tregs and NK cells. *JCI Insight.* 2016;1:e89278.
- Cantilena CR, Ito S, Tian X, et al. Distinct biomarker profiles in ex vivo T cell depletion graft manipulation strategies: CD34<sup>+</sup> selection versus CD3<sup>+</sup>/19<sup>+</sup> depletion in matched sibling allogeneic peripheral blood stem cell transplantation. *Biol Blood Marrow Transplant.* 2018;24:460–466.
- Kong Y, Zhang J, Claxton DF, et al. PD-1(hi)TIM-3(+) T cells associate with and predict leukemia relapse in AML patients post allogeneic stem cell transplantation. *Blood Cancer J.* 2015;5:e330.
- Norde WJ, Maas F, Hobo W, et al. PD-1/PD-L1 interactions contribute to functional T-cell impairment in patients who relapse with cancer after allogeneic stem cell transplantation. *Cancer Res.* 2011;71:5111–5122.
- Oostvogels R, Lokhorst HM, Mutis T. Minor histocompatibility Ags: identification strategies, clinical results and translational perspectives. *Bone Marrow Transplant.* 2016;51:163–171.
- Gros A, Parkhurst MR, Tran E, et al. Prospective identification of neoantigen-specific lymphocytes in the peripheral blood of melanoma patients. *Nat Med.* 2016;22:433–438.
- Tran E, Robbins PF, Rosenberg SA. 'Final common pathway' of human cancer immunotherapy: targeting random somatic mutations. *Nat Immunol.* 2017;18:255–262.
- Woo SR, Li N, Bruno TC, et al. Differential subcellular localization of the regulatory T-cell protein LAG-3 and the coreceptor CD4. *Eur J Immunol.* 2010;40:1768–1777.